A self-consistent model of the interacting ring current ions and electromagnetic ion cyclotron waves, initial results: Waves and precipitating fluxes

G. V. Khazanov,[1] K. V. Gamayunov,[2] V. K. Jordanova,[3] and E. N. Krivorutsky[2]

Received 19 June 2001; revised 28 November 2001; accepted 28 November 2001; published 26 June 2002.

[1] Initial results from a newly developed model of the interacting ring current ions and ion cyclotron waves are presented. The model is based on the system of two kinetic equations: one equation describes the ring current ion dynamics, and another equation describes wave evolution. The system gives a self-consistent description of the ring current ions and ion cyclotron waves in a quasilinear approach. These equations for the ion phase space distribution function and for the wave power spectral density were solved on aglobal magnetospheric scale under nonsteady state conditions during the 2–5 May 1998 storm. The structure and dynamics of the ring current proton precipitating flux regions and the ion cyclotron wave-active zones during extreme geomagnetic disturbances on 4 May 1998 are presented and discussed in detail. *INDEX TERMS:* 2736 Magnetospheric Physics: Magnetosphere/ionosphere interactions; 2708 Magnetospheric Physics: Current systems (2409); 2753 Magnetospheric Physics: Numerical modeling; 2730 Magnetospheric Physics: Magnetosphere—inner; *KEYWORDS:* ring current, inner magnetosphere, plasmasphere, numerical modeling

1. Introduction

[2] Low-frequency Alfvén, fast magnetosonic, and ion cyclotron waves (ICWs) are commonly found in space plasmas. One example is ICWs in Earth's ring current (RC) region [e.g., *LaBelle et al.*, 1988; *Anderson et al.*, 1992a, 1992b]. ICWs have also been observed at geostationary orbit [*Young et al.*, 1981; *Mauk*, 1982, and references therein], in the outer magnetosphere [*Anderson et al.*, 1990, 1992a, 1992b], at high latitudes [*Erlandson et al.*, 1990], and at ionospheric altitudes [*Iyemori and Hayashi*, 1989].

[3] Low-frequency waves (LFWs) in the ICW mode can effectively interact with different components of the magnetospheric plasma through heating and acceleration [e.g., *Gendrin*, 1985]. Such LFWs are believed to be responsible for precipitation of the RC protons [*Kennel and Petschek*, 1966], formation of stable auroral red arcs [*Cornwall et al.*, 1971], and acceleration of heavy ions [*Omura et al.*, 1985; *Tanaka*, 1985]. The transport of the dissipating wave energy, from the plasmasphere along the geomagnetic field lines into the ionosphere below, could account for the observed subauroral rise in the electron temperature [e.g., *Kozyra et al.*, 1987, and references therein]. LFWs can also interact with magnetospheric plasma due to nonlinear coupling of Alfvén and lower hybrid waves [*Khazanov et al.*, 1996, 1997a, 1997b, 2000] and due to formation of nonlinear Alfvénic structures in the RC region [*Gamayunov and Khazanov*, 1995].

[4] The effect of ICWs, generated by the positive ion temperature anisotropy [e.g., *Kennel and Petschek*, 1966; *Lyons and Williams*, 1984], on Earth's RC dynamics is one of the best known examples of wave-particle interaction in the magnetosphere. The temperature anisotropy is the source of free energy needed to generate ICWs, and for a bi-Maxwellian phase space distribution, function is introduced as $A = T_\perp/T_\parallel - 1$; here $T_\perp$ and $T_\parallel$ are RC ion temperatures transverse to and along the geomagnetic field, respectively. In spite of numerous theoretical studies related to the RC-ICW interaction, some questions still remain unsolved and can be answered only in the framework of a quasilinear self-consistent treatment of the waves and RC ions. One group of the questions is related to the ICWs itself; for example, spatial/temporal generation, evolution, and decay of the waves along with their spectral characteristics such as frequency, wave-normal angle, and form of the power spectral density. To answer these questions properly, in addition to the RC kinetic equation, the wave-kinetic equation should also be employed. One example is that in order for the strong nonlinear wave phenomena to take place in the RC region, the ICW energy should exceed some thresholds [e.g., *Gamayunov et al.*, 1992; *Khazanov et al.*, 1996, 1997a, 1997b, 2000; *Gamayunov and Khazanov*, 1995, and references therein], so the wave energy should be known precisely. We anticipate that a quasilinear self-consistent description mostly produces a realistic wave energy distribution that could be used to predict localization of the strong ICW nonlinearity in Earth's magnetosphere. Another group of unanswered questions is associated with the RC evolution under the influence of ICW activity. Resonant interaction of ICWs and RC ions is sensitive to

[1]NASA, Marshall Space Flight Center, Huntsville, Alabama, USA.
[2]Geophysical Institute, University of Alaska, Fairbanks, Alaska, USA.
[3]Space Science Center, University of New Hampshire, Durham, New Hampshire, USA.

0148-0227/02/2001JA000180$09.00

both particle and wave parameters. This sensitivity may play a critical role in determining the RC ion loss rate. During the main storm phase the RC decay due to resonant interaction with ICWs can be substantially faster than decay due to charge exchange or Coulomb scattering because starting with a certain level of the wave energy, this interaction causes strong diffusion of the RC ions directly into the loss cone [*Gonzalez et al.*, 1994]. One more example supporting a self-consistent approach arises owing to pitch angle dependences of both charge exchange and resonant RC-ICW interaction. The RC charge exchange lifetime strongly increases with the pitch angle increase [e.g., *Ebihara and Ejiri*, 2000]. The pitch angle anisotropy produced by the charge exchange results in an ion phase space distribution function that is unstable to the excitation of ICWs. However, RC-ICW interaction moves ions from the region of large pitch angles to the boundary of the loss cone, i.e., supplies RC ions to the pitch angle region of a more effective charge exchange. This dynamic and delicate process may speed up the RC decay depending on the power of ICWs and should be described self-consistently.

[5] Recently, using quasilinear kinetic equation on a global scale, *Jordanova et al.* [1997] addressed RC loss due to resonant interaction between particles and ICWs. The spatial regions of ICW instability were determined by first calculating the convective growth rates from the dispersion relation in a bi-Maxwellian plasma and using the RC characteristics as supplied by the model, integrating the convective growth rates along the field-aligned wave paths, and then selecting the regions of maximal wave amplification. It was found that source regions are located in the duskside magnetic local time (MLT) sector in agreement with the predominant occurrence of ICWs. The fluctuating field of ICWs was regarded as imposed on the system, and wave-particle interaction was described as a diffusive process. The multi-ion quasilinear diffusion coefficient [*Jordanova et al.*, 1996] was then included in the calculation, assuming within the unstable regions the spectral power density of 1 nT^2/Hz, which is consistent with AMPTE/CCE observations of Pc 1–2 [*Anderson et al.*, 1992a, 1992b]. Further, *Jordanova et al.* [1998b, 2001] developed the model including RC energy diffusion, caused by the wave-particle interaction, and used a semiempirical model to relate the calculated wave gains to the wave amplitudes.

[6] The above mentioned studies of wave-particle interaction were not self-consistent; that is, the unstable regions of the magnetosphere were predetermined by results from a calculation of convective growth rates in a bi-Maxwellian plasma. A semiempirical approach to obtain wave energy density was used, and the form of wave power spectral density was assumed to be Gaussian. But it is well known that the effects of ICWs on RC ion dynamics strongly depend on such assumed particle/wave characteristics as the ion phase space distribution function, frequency, wave-normal angle, wave energy, and the form of wave spectral energy density, so all of these characteristics should be properly determined by the wave-ion evolution itself. So to quantify the ICW effects on the RC ion dynamics, a self-consistent theoretical description of the ions and waves is employed in this study. We present the first results from a newly developed RC model that self-consistently simulates generation, evolution, and damping of the waves in a dynamic plasmasphere along with RC ion dynamics. We simultaneously solved the RC and wave-kinetic equations. The effects on RC ions interacting with ICWs, and back on the waves, have been considered self-consistently, calculating the RC-ICW relationships on a global magnetospheric scale under nonsteady state conditions. Interaction of ICWs with RC ions mainly causes pitch angle scattering and moves ions into the loss cone. The energy diffusion due to wave-particle interaction has a smaller effect due to the smaller diffusion coefficient, and we neglect this process in the present study. (The energy diffusion due to RC-ICW interaction will be taken into account in the course of further model development.)

[7] One of the most pronounced manifestations of the RC evolution is an ion precipitation at low altitudes. The intensity of ion precipitation varies with storm development and is controlled globally by the magnetospheric convection electric field. The precipitation fluxes increase during the main phase of the storm owing to enhancement of the convection electric field, and they decrease during the storm recovery when the convection electric field subsides. In addition to RC precipitation due to the convection electric field, Coulomb scattering and resonant interaction with ICWs also contribute to the increase of the precipitating ion fluxes. Coulomb scattering of RC ions can become an important loss process along the inner edge of the RC. The role of pitch angle scattering due to RC-ICW interaction during the early recovery phase of the 4 November 1993 large magnetic storm was studied by *Kozyra et al.* [1997], who found that wave-induced RC precipitation is an important contribution to the total RC decay during this storm phase.

[8] In the course of our current investigation we produced the global patterns of the ICW distributions and the RC proton precipitating fluxes during the 2–5 May 1998 storm. In this paper we only present the data obtained during extreme geomagnetic disturbances on 4 May 1998 along with discussion of the structure and dynamics of the precipitating flux regions and of the wave-active zones.

2. Model

[9] We simulate the RC dynamics by solving the bounce-averaged kinetic equation for the phase space distribution function, Q, of the RC species,

$$\frac{\partial Q}{\partial t}+\frac{1}{R_0^2}\frac{\partial}{\partial R_0}\left(R_0^2\left\langle\frac{dR_0}{dt}\right\rangle Q\right)+\frac{\partial}{\partial\varphi}\left(\left\langle\frac{d\varphi}{dt}\right\rangle Q\right)+\frac{1}{\sqrt{E}}\frac{\partial}{\partial E}\cdot\left(\sqrt{E}\left\langle\frac{dE}{dt}\right\rangle Q\right)+\frac{1}{\mu_0 h(\mu_0)}\frac{\partial}{\partial\mu_0}\left(\mu_0 h(\mu_0)\left\langle\frac{d\mu_0}{dt}\right\rangle Q\right)=\left\langle\left(\frac{\delta Q}{\delta t}\right)_{\text{loss}}\right\rangle, \quad (1)$$

as a function of position in the magnetic equatorial plane (R_0, φ); kinetic energy and the cosine of the equatorial pitch angle (E, μ_0); and time t. In the left-hand side of this equation all of the bounce-averaged drift velocities are denoted as $\langle\cdots\rangle$. The term on the right-hand side of equation (1) includes losses from charge exchange, Coulomb collisions, ion-wave scattering, and precipitation at low altitudes. Loss through the dayside magnetopause is taken

into account, allowing free outflow of the RC ions from the simulation domain. (For more details regarding equation (1), see *Jordanova et al.* [1997, and references therein].) The ion-wave collisional term, included in the right-hand side of equation (1), is a function of ICW power spectral density that may be obtained from the wave-kinetic equation. ICWs propagate along the geomagnetic field lines and reflect at ionosphere altitudes, bouncing between conjugate ionospheres. Averaging the wave-kinetic equation over a period of the "fast" wave bounce oscillations, we can obtain the equation to describe "slow" evolution of the wave power spectral density. Following *Bespalov and Trakhtengerts* [1986], the equation can be presented as

$$\frac{\partial\left\langle B^2_{\omega,\theta}\right\rangle}{\partial t} = \left(\ln R + 2\oint \frac{\gamma}{v_g} ds\right)\frac{\left\langle B^2_{\omega,\theta}\right\rangle}{T_s}, \qquad (2)$$

where $\langle B^2_{\omega,\theta}\rangle = \langle B^2(\omega, \theta, \varphi, R_0)\rangle$ averaged over wave bounce oscillation; ω is a wave frequency; and θ is the angle between the external magnetic field line and the wave vector. Parameter R is the effective reflection coefficient from the ionosphere characterizing wave energy loss due to nonperfect reflection. The local wave growth rate, $\gamma(\omega, \theta, \varphi, R_0, s)$, which depends on the phase space distribution function of the RC species, should be averaged over bounce oscillation of the wave envelope. The factor $T_s/2$ is the time of group propagation of the wave signal between conjugate ionospheres, and v_g is a wave group velocity.

[10] To obtain equation (2), we neglected slow longitudinal and radial drifts of ICWs and change of the wave-normal vector orientation during ICW bounce oscillation [*Bespalov and Trakhtengerts*, 1986]. It should be noted that γ includes contribution not only from the ICW growth due to interaction with RC ions but also from the ICW damping due to absorption by the core plasma particles (i.e., γ may change its sign). The right-hand side of the kinetic equation (1) depends on ICW energy density, and γ in equation (2) is determined by the phase space distribution function Q. The resulting system of equations (1) and (2) gives a self-consistent description of the interacting RC ions and ICWs in a quasilinear approach.

[11] Equation (2) should be accompanied by the model of reflection index calculation. We incorporate the global reflection model into the RC-ICW interaction model; to the best of our knowledge this approach has not been used before. The general expression for the ICW reflection index was obtained by *Lyatsky and Mal'tsev* [1983]. The reflection index depends on both spectral wave and ionosphere parameters. Ionospheric properties affect the reflection index through the integral Pedersen and Hall conductances. In our simulation we adopted analytical conductivity models of both Pedersen and Hall conductances [*Simons et al.*, 1985]. These models are based on 4 years of measurements of precipitating particle fluxes from Atmosphere Explorer C and D. For each 1-hour MLT bin, there is a Gaussian curve versus invariant latitude. The Gaussian parameters are governed by the *AE* index. The location and magnitude of the Gaussian peak were found to be linear in *AE*, whereas the width of the peak was found to be nearly independent of *AE*. So each of the Pedersen and Hall conductivity models depends on 120 parameters (5 constants define Gaussian fits for 24 MLTs) and the *AE* index.

[12] To solve kinetic equation (1), we rewrite it in the conservative form and employ the "time-splitting" method [*Yanenko*, 1971]. The advantage of the splitting method is that the multidimensional problem is split into a sequence of one-dimensional problems. For each time step we could obtain an approximate solution to the multidimensional problem by consecutively solving several one-dimensional problems using the result obtained from the previous one as the initial condition for each following problem. The order of the solution operators is reversed during the next time step to achieve second-order accuracy in time. The first-order advective terms due to drifts and Coulomb drag energy degradation are solved using a high-resolution method that combines the second-order Lax-Wendroff scheme with the first-order upwind scheme via a superbee flux limiter [*LeVeque*, 1992]. Analytical solutions for the charge exchange and the atmospheric loss terms, and also for the wave-kinetic equation (2), are used at each time step. The pitch angle diffusion terms due to Coulomb scattering and wave-ion interaction are solved with the Crank-Nicolson scheme [e.g., *Potter*, 1973]. This scheme is an implicit algorithm which is second-order accuracy in both pitch angle and time.

[13] The geomagnetic field, B, used in our simulation is taken to be a dipole field. The electric field is expressed as the Volland-Stern-type convection field [*Volland*, 1973; *Stern*, 1975], which is *Kp* dependent, and as a corotation field. The plasmaspheric cold electron density, N_e, is calculated with the time-dependent equatorial model of *Rasmussen et al.* [1993]. To calculate the wave characteristics, we also employ a three-dimensional model of the core plasma density of *Angerami and Thomas* [1964], which is adjusted to the *Rasmussen et al.* [1993] model at the equator. Geocoronal hydrogen densities, used to calculate loss due to charge exchange, are obtained with the model of *Rairden et al.* [1986].

[14] In the present model the equatorial simulation domain is from $L = 2$ to 6.5 and covers all MLTs. The energy domain is 0.01–430 keV, and the pitch angle range is only 0–90° because the phase space distribution function is assumed to be symmetric about a 90° pitch angle. To obtain initial conditions, the simulation was started at 0000 UT on 1 May 1998 using background noise level for ICWs [*Akhiezer et al.*, 1975] and the statistically derived quiettime distribution of *Sheldon and Hamilton* [1993] for the RC protons. The nightside boundary conditions are updated during the storm evolution using flux measurements from the Magnetospheric Plasma Analyzer and Synchronous Orbit Particle Analyzer instruments on the geosynchronous Los Alamos National Laboratory satellites. In ~20 hours the wave magnetic energy distribution reaches quasistationary state, indicating that the RC-ICW system achieves a quasi self-consistent state. So the self-consistent modeling of the May 1998 storm period is started at 0000 UT on 2 May using solutions of the equations (1) and (2) at 2400 UT on 1 May as the initial conditions. At this time the typical wave magnetic field amplitudes are of order 1 nT or less.

3. Results and Discussions

[15] The interplanetary configuration of 1–5 May 1998 consists of a coronal mass ejection (CME) interacting with a trailing faster stream [*Farrugia et al.*, 2001]. The CME drives an interplanetary shock observed by the instruments

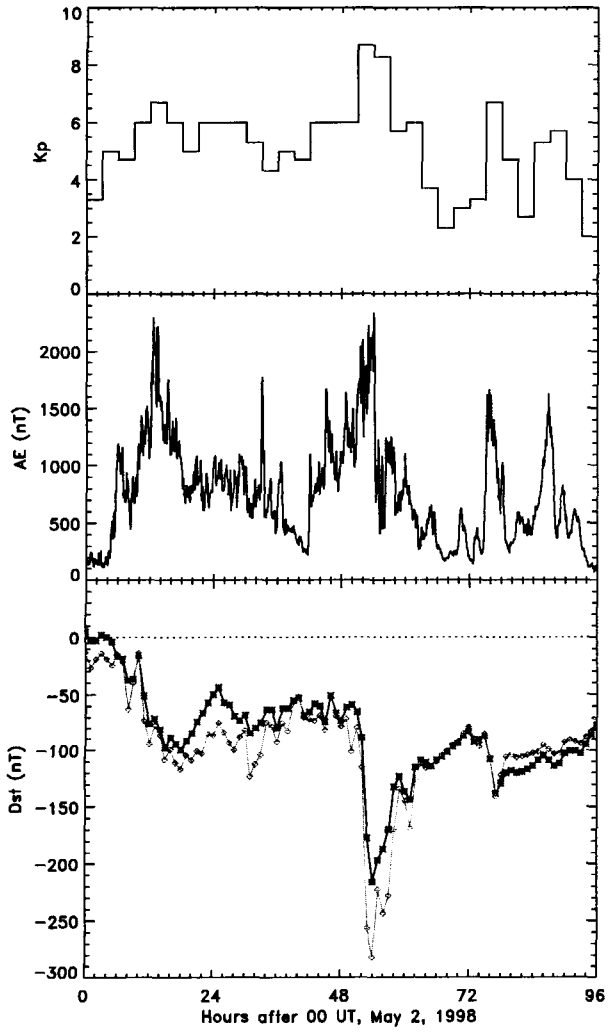

Figure 1. Geomagnetic indices for the 2–5 May 1998 storm period. (top) Three-hour *Kp* index. (middle) *AE* index. (bottom) *Dst* index. Stars depict measured *Dst*, and blue diamonds mark quiettime magnetopause current corrected *Dst**.

on Wind spacecraft at ~2200 UT on 1 May. Two periods of a strongly negative north-south IMF component are monitored: The first at ~0400 UT on 2 May and the second at ~0200 UT on 4 May. These caused a "double-dip" storm with a minimum *Dst* = −100 and −215 nT, respectively. The magnetopause current correction to *Dst* is largest near 0600 UT on 4 May. The measured (pressure corrected) *Dst* index during 2–5 May 1998 is shown with stars (diamonds) in the bottom panel of Figure 1. The planetary Kp index reached maximum values $Kp \approx 7^-$ and 9^- at the times when minimum Dst were recorded (Figure 1, top). The AE index during 2–5 May 1998 is shown in the middle panel of Figure 1. Several peaks are seen, with maximum $AE \sim 2300$ nT, corresponding to the maximums of *Kp* value. An initial study of RC development during this storm period was presented by *Farrugia et al.* [2001]. These authors have used the RC kinetic model of *Jordanova et al.* [1998a] to model *Dst* variation during the storm and to calculate energy content for the major RC ion species: H^+, O^+, and He^+. They found that during this storm the energy density of H^+ is greater than twice that of O^+ at all MLTs, and the contribution of He^+ to the RC energy content is negligible. This result allows us to assume that the RC is entirely made up of energetic protons and to neglect the He^+ and O^+ RC ions in the simulation.

[16] One of the most pronounced manifestations of the RC-ICW interaction is an ion precipitation at low altitudes. We obtain a global storm history in the terms of squared wave magnetic field,

$$B_w^2 = \int_{\omega_{min}}^{\omega_{max}} d\omega \int_0^{\pi} d\theta \left\langle B_{\omega,\theta}^2 \right\rangle, \tag{3}$$

and RC proton precipitating fluxes,

$$J_{lc} = \frac{1}{\Omega_{lc}} \int_{E_1}^{E_2} dE \int_{\mu_{lc}}^{1} d\mu_0 j, \qquad \Omega_{lc} = \int_{\mu_{lc}}^{1} d\mu_0, \tag{4}$$

where μ_{lc} is the cosine of the equatorial pitch angle at the boundary of loss cone and j is an ion differential flux. Geomagnetic disturbances reach extreme during the 4 May 1998 storm period. Figures 2, 3, and 4 refer to 1600 UT on 3 May, to 0600 UT on 4 May, and to 2000 UT on 4 May, respectively. Generation of ICWs strongly depends on

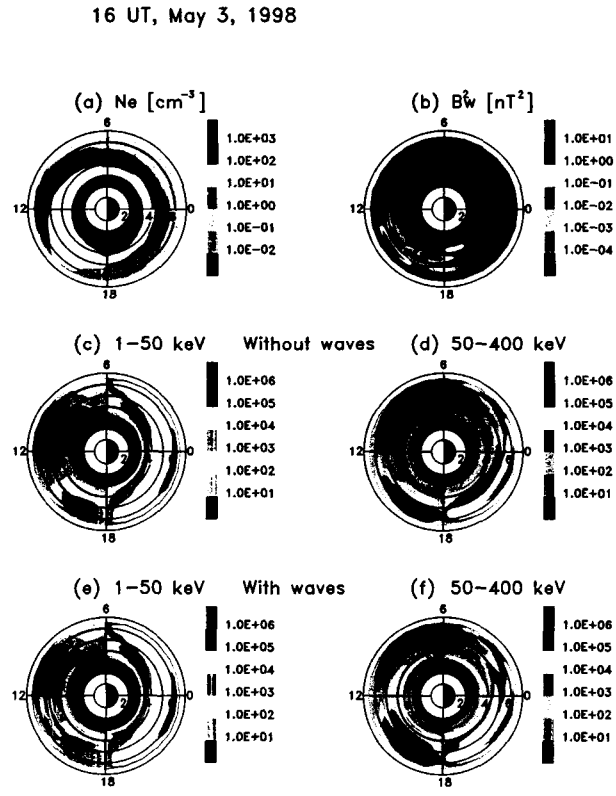

Figure 2. Results of a self-consistent RC-ICW simulation at 1600 UT on 3 May. (top) Equatorial plasmaspheric electron density and square of ICW magnetic field as (MLT, *L* shell) functions. Figures 2c, 2d, 2e, and 2f show RC proton-precipitating fluxes integrated over two energy ranges and averaged over equatorial loss cone in $cm^{-2}\,s^{-1}\,sr^{-1}$. (middle) Without wave-particle interaction and (bottom) wave-particle interaction is included.

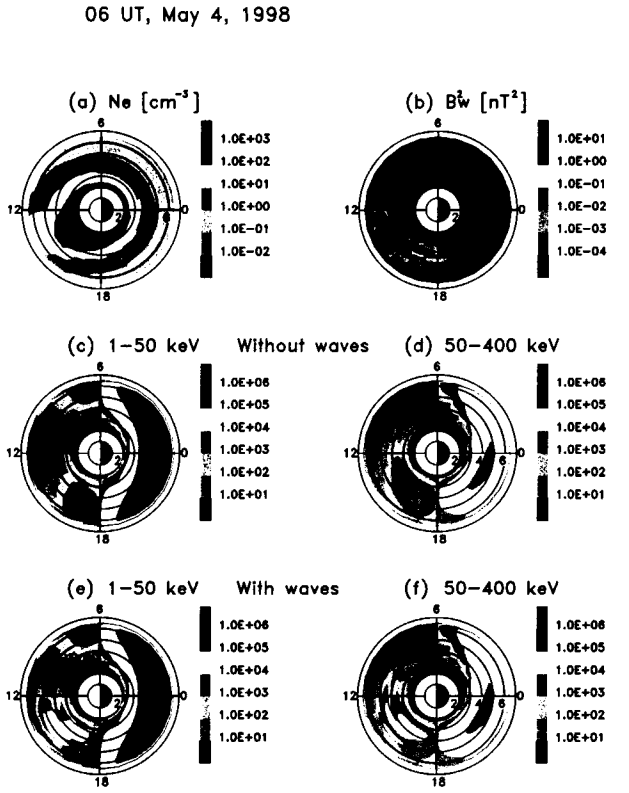

Figure 3. The same as in Figure 2 at 0600 UT on 4 May.

plasmaspheric core plasma density. To demonstrate this effect, Figures 2, 3, and 4 include not only squared wave magnetic field and RC proton precipitating fluxes but also equatorial plasmaspheric electron density as a function of L shell and MLT. The most intense wave generation takes place around the plasmaspheric bulge (the most extended part of the plasmapause, which does not necessarily occur in the dusk MLT sector). In the present study we identify the region of the most intense wave generation with the current (MLT, L shell) positions of the maximal wave growth rates. It is not necessary that this region coincides with the region of the strongest ICWs at this time. In the electron density snapshots the plasmaspheric bulge may be approximately identified with the most extended transitional region between the red and yellow colors. The above feature of the wave generation is well known and is due to the fact that kinetic energy of the resonating RC protons, $E_{\|} \sim B^2/(8\pi N_e)$, reaches minimum near the plasmaspheric bulge, and the number of resonating ions decreases with energy increase [*Lyons and Williams*, 1984]. In the equatorial plane the radial extent of the region of most intense waves (from $\sim$1 up to $\sim$10 nT) may reach two Earth radii centered on the plasmapause. The MLT size of this region depends on the form and position of the plasmaspheric bulge. Basically, the size is 2–5 hours, but of course, less-intense wave regions are more extended. As the storm evolves, the plasmaspheric bulge changes its position and form. It causes migration of the wave generation region and wave damping in the region of the former bulge position. (There is wave damping due to nonideal reflection from the ionosphere and to absorption by the core plasma.)

[17] Pitch angle scattering, caused by the RC-ICW interaction, moves protons into the loss cone. This diffusion process reduces pitch angle anisotropy of the ions and growth rate of the ICWs. The level of wave energy density in the active zone depends on strengths of the wave sources and of the wave sinks. If wave damping due to nonperfect reflection from the ionosphere and due to absorption by the plasmaspheric core plasma exceeds generation rate, ICWs damp. Damping time may be estimated as the typical time of wave energy loss due to the above energy loss mechanisms. During the 2–5 May 1998 storm period, this time was an order of a few hours (sometimes a little more than 10 hours). At the same time, MLT drift of the resonating RC protons takes place with a rate of the same order of magnitude. This drift supplies an ion population with "fresh" phase space distribution function into the unstable region and changes the above local damping rate.

[18] During the initial phase of the 4 May 1998 storm period (Figure 2), ICW activity is concentrated in the postnoon to dusk MLT sector with a wide radial extent from $L = 3.75$ up to 5.75. The observed (MLT, L shell) shape of the wave-active zone is mostly the result of previous RC wave evolution. The plasmaspheric bulge was localized in the postnoon to dusk MLT sector, between $L \sim 4$ and $\sim$5.5, during the time period from 0000 UT on 2 May until 1600 UT on 3 May. Not shown is the snapshot at 1200 UT on 3 May 1998 that demonstrates practically the same shape of the wave-active region as in Figure 2b but with more developed wave activity. In this "result of previous evolution" region the maximal wave amplitude of $\sim$5 nT is observed around

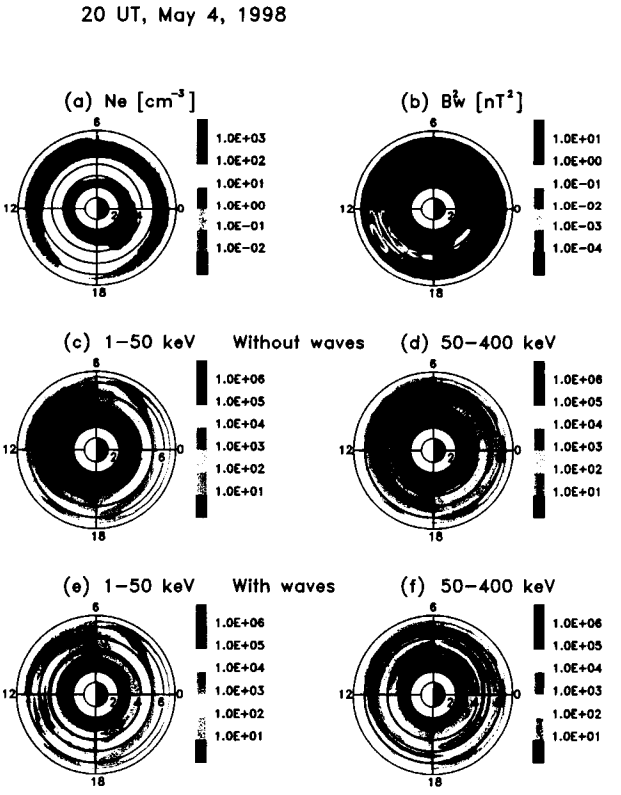

Figure 4. The same as in Figure 2 at 2000 UT on 4 May.

$L = 5$, MLT = 16 (see Figure 2b). Only one small spot, slightly eastward of the current (at 1600 UT) bulge position, is a newly appeared wave zone. This new zone is centered at $L = 3.75$, MLT = 19, and is identified with the bulge position. In spite of ICWs growing in this new region, their current wave amplitude is only 0.8 nT, which is much less than in the damping "result of previous evolution" wave zone. Further, until ~2200 UT on 3 May the plasmasphere was found to be almost the same except the plasmaspheric bulge was slightly drifting sunward and waves were gradually damping. In the time cut at 2200 UT on 3 May (not shown), the wave-active region is shrunken in both radial ($L = 3.75-5$) and azimuthal (MLT = 15–18) directions and has the dappled structure. Wave amplitudes at this time are much less than in Figure 2b and are mostly ~0.1 nT. Only in one tiny spot the wave amplitude is 1.8 nT (this spot is localized near $L = 5$, MLT = 16 and is a "residue" of the most intense waves in Figure 2b). So the wave-active region in Figure 2b practically disappears in 6–7 hours.

[19] Figure 3 presents the main phase of the studied storm period. During this phase the plasmasphere is extremely compressed, the plasmaspheric bulge reverts into the postnoon to dusk MLT sector, and the wave activity is highly developed. Intense ICWs exhibit very "dense" (MLT, L shell) distribution, and they are organized well around the plasmaspheric bulge. In comparison with the initial storm phase the most active region moves much closer to noon, and the major part of the postnoon to dusk MLT sector, with a radial extent from $L = 3.5$ up to 6, confines very intense ICWs. Waves in the vicinity of $L = 4$, MLT = 16 have maximal amplitude of ~8 nT. Strong feedback between the waves and the resonating RC protons reduces the ICW growth rate and results in fast wave damping. For example, the wave pattern at 0800 UT on 4 May (not shown) looks more shrunken and less intense than 2 hours before. Figure 4 refers to the late recovery phase of the discussed storm period. The wave-active region occupies almost all of the noon to midnight MLT sector. In this snapshot the former active region observed in Figure 3b is shrunken, especially at its inner edge, and depressed (maximal wave amplitude is < 2 nT). During this recovery phase the plasmasphere becomes more symmetric, and the newly generated ICWs follow the plasmaspheric bulge and reach premidnight MLTs with a radial extent from $L = 3.75$ up to 4.5. Maximal wave amplitude of ~7 nT is found just a little sunward of the bulge near $L = 4.5$ and MLT = 19.

[20] To demonstrate RC proton precipitating fluxes, Figures 2, 3, and 4 include fluxes integrated over two energy ranges, 1–50 and 50–400 keV, and also averaged over equatorial loss cone. Both results with and without wave-particle interaction are presented. Results without the RC-ICW interaction were obtained by solving only a single equation (1) with wave energy density set to zero, and results with RC-ICW interaction follow from the system of two equations (1) and (2). Figure 2 refers to the initial phase of the 4 May 1998 storm period with $Kp = 5$. As RC protons approach Earth via the convection electric field, they precipitate into the loss cone because the equatorial loss cone angle increases with decreasing L shell somewhat more than the equatorial pitch angle increases [e.g., *Jordanova et al.*, 1997]. The most intense precipitating fluxes take place in the nightside MLT sector, and maximal values of ~10^5 cm^{-2} s^{-1} sr^{-1} are found in both energy channels. In the dayside magnetosphere the precipitating fluxes are diminished because of the proton drift out of the loss cone; that is, there is no more ion source at the boundary of the loss cone. From Figures 2c and 2d we can see that protons of the energies 50–400 keV drift westward for radial distances < L = 6.5 because there are no precipitating fluxes seen from the nightside through the dawn MLT boundary, whereas in the lower energy channel, 1–50 keV, we observe both eastward and westward drifts. Figures 2e and 2f show first of all, that the wave activity causes a local increase of precipitating fluxes. Another noticeable feature of the RC-ICW interaction is a nonlocal wave effect on the precipitating fluxes; that is, there are flux increases out of the wave-active region. This effect is most pronounced in the high-energy channel. It follows from comparison of Figures 2f and 2d that the major portion of the ion trajectories crossing the wave-active region is composed of the closed drift trajectories. (Of course, this conclusion from Figures 2f and 2d is only reliable regarding the resonating protons, i.e., mostly for particles from the low-energy end of the energy range. Note that probably the high-energy end ions also go along the closed trajectories because the higher the ion energy, the more radially extended their closed trajectories.) In the dusk MLT sector the last closed drift trajectory position is near $L = 5$, and there are open drift trajectories for the bigger L shells. After the drifting RC protons leave the wave-active region, they cannot precipitate into the loss cone due to scattering on the waves, but their phase space distribution function should be enriched in the vicinity of the boundary of the loss cone. Indeed, this fact is supported by the results of our simulation presented in Figure 5 for two proton energies. Figure 5 demonstrates the proton trapped fluxes around $L = 4.5$, MLT = 11 at 1600 UT on 3 May 1998 versus the equatorial pitch angle. As we can see in the vicinity of the loss cone boundary, after passing the wave-active zone the proton-trapped fluxes are approxi-

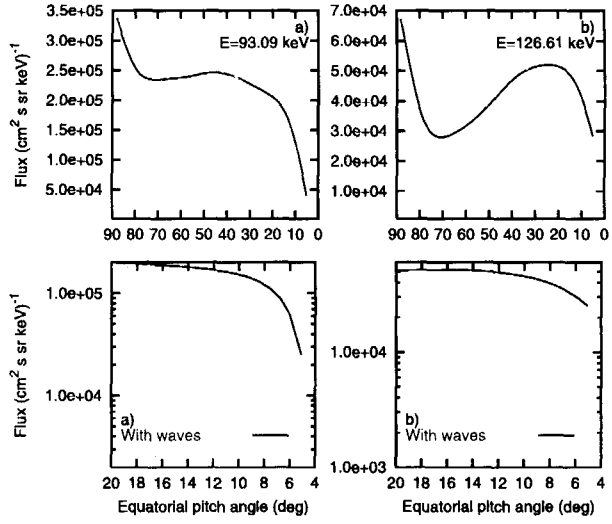

Figure 5. The modeled RC proton trapped fluxes obtained in the equatorial plane at $L = 4.5$, MLT = 11 at 1600 UT on 3 May 1998. Both results with and without wave-particle interaction are presented in two different scales. Equatorial loss cone angle is 4.67°. (a and b) Results for the two different proton kinetic energies.

mately one order of magnitude higher than in the case of no RC-ICW interaction. If the ions in the vicinity of the loss cone boundary drift along the closed trajectories, they will precipitate later, somewhere in the nightside MLT sector, due to the earthward drift. This pattern is well observed in Figure 2f (compare it with Figure 2d) as a flux enhancement in the wide radial range from $L = 3.5$ up to $L = 5.5$. In the low-energy channel, as follows from Figures 2c and 2e, almost all drift trajectories of the resonating ions are open, and precipitating flux is only locally enhanced in the wave-active MLT sector.

[21] The main phase of the storm period is presented in Figure 3. Growth of the magnetospheric convection electric field, $Kp = 8.3$, significantly increases the ion flux to the boundary of the loss cone as the RC protons approach Earth. As a consequence, precipitating fluxes are strongly enhanced almost everywhere in the nightside MLT sector. In comparison with Figures 2c and 2d the inner edges of intense fluxes are much closer to Earth. While the last closed equipotential lines are more shrunken than during the initial storm phase, protons of energies 50–400 keV still drift westward for radial distances $< L = 6.5$. In Figure 3c we observe a highly west-east symmetry in the nightside precipitating flux distribution. This picture is formed by the protons drifting mainly due to the convection electric field, i.e., along their open drift trajectories. The magnitudes of the most intense precipitating fluxes are $\sim 3 \times 10^5$ cm^{-2} s^{-1} sr^{-1} and 10^5 units in the low- and high-energy channels, respectively. During this phase the wave activity is highly developed and causes strong local enhancement of the precipitating fluxes. In the wave-active regions the maximal fluxes have magnitudes of $\sim 6 \times 10^4$ cm^{-2} s^{-1} sr^{-1} and 3×10^4 units in the low- and high-energy channels, respectively. Dayside precipitating flux snapshots are qualitatively the same as for the initial storm phase except (1) last closed drift trajectories are more shrunken, and (2) outflow rate of the RC protons away from the loss cone boundary is enhanced during the main phase (compare Figures 3c, 3d, 3e and 3f with Figures 2c, 2d, 2e and 2f).

[22] The late recovery phase of the discussed storm period is demonstrated in Figure 4. Because the convection electric field at this time is reduced ($Kp = 2.8$), the precipitating flux snapshots look somewhat poor. The inner edges of the fluxes recede to the shells $L \sim 4$ (see Figures 4c and 4d). In the low-energy channel we see eastward drift only for the radial distances above $L \approx 5.5$. The magnitudes of the most intense precipitating fluxes are $\sim 6 \times 10^4$ cm^{-2} s^{-1} sr^{-1} and 10^4 units in the low- and high-energy channels, respectively. While during this recovery phase the wave activity is not as strong as before, it is still high enough, and waves occupy the large region in the noon to premidnight MLT sector. Wave activity causes both local and nonlocal enhancements of precipitating fluxes and extends the region of precipitation radially in both directions. These effects are clearly observed in Figures 4e and 4f. The highest magnitudes of the precipitating fluxes, induced by ICWs in both energy channels, are just a little less than 10^4 cm^{-2} s^{-1} sr^{-1}.

4. Conclusions

[23] The effect of ICWs, generated by the ions with temperature anisotropy, on Earth's RC is one of the important and the best-known examples of wave-particle interaction in the magnetosphere. Numerous studies related to this subject were based on the prescribed wave characteristics. Partly due to the use of this semiphenomenological approach, a number of questions (in particular, these related to the RC loss processes) still remain unsolved. It is known that the effects of ICWs on RC ion dynamics strongly depend on the particle/wave characteristics such as the ion phase space distribution function, frequency, wave-normal angle, wave energy, and the form of the wave power spectral density. Therefore the answers to some unsolved questions are possible only in the framework of wave and particle self-consistent treatment [*Gonzalez et al.*, 1994].

[24] In this paper we presented the first results from a newly developed self-consistent RC model, which simulates generation, evolution, and damping of the waves in a dynamic plasmasphere along with RC ion dynamics. We solved the system of two kinetic equations. The system includes equation (1) for the RC ions and equation (2) for the ICWs. The right-hand side of equation (1) depends on ICW energy density, and γ in equation (2) is determined by the RC phase space distribution function. Such a system gives a self-consistent description of the interacting RC ions and ICWs in a quasilinear approach. Calculating the RC-ICW relationships on a global magnetospheric scale during the 2–5 May 1998 storm, we presented the data obtained during extreme geomagnetic disturbances on 4 May 1998; there are snapshots during the initial (1600 UT on 3 May), main (0600 UT on 4 May), and late recovery (2000 UT on 4 May) phases of this storm period. The structure and dynamics of the RC proton precipitating flux regions and the wave-active zones were discussed in detail.

[25] Presented results of the self-consistent simulation of the 4 May 1998 storm period may be summarized as follows:

1. The strongest wave generation takes place along the plasmaspheric bulge because the kinetic energy of the resonating RC protons, $E_{||} \sim B^2/(8\pi N_e)$, reaches a minimum near the bulge. In the equatorial plane the radial extent of the regions of most intense waves (from ~ 1 nT up to ~ 10 nT) may reach two Earth radii centered on the plasmapause. The MLT size of these regions depends on the form and position of the plasmaspheric bulge and basically is 2–5 hours.

2. If the wave-damping rate due to nonperfect reflection from the ionosphere and due to absorption by the plasmaspheric core plasma exceeds the generation rate, ICWs damp with a typical time ranging from a few to ~ 10 hours. This local damping is altered by the MLT drift of the resonating RC protons and by evolution of the plasmaspheric bulge. (MLT drift supplies "fresh" ion population into the unstable region, and evolution of the plasmaspheric bulge causes migration of the wave generation region and wave damping in the region of the former bulge position.)

3. During the studied storm period the region of ICW activity occupies the noon to premidnight MLT sector and is highly changeable in radial and MLT extents depending on the storm phase. The most intense ICWs of ~ 8 nT are found in the postnoon to dusk MLT sector during the main phase of the storm period.

4. ICW activity leads to enhancements of the precipitating fluxes that are both (1) local, i.e., inside the wave-active region, and (2) nonlocal, i.e., outside the wave-active region, and even in the nightside sector. The significance of the nonlocal effect depends on the type of drift trajectories of the resonating ions (closed or open trajectories) and the strength of both magnetospheric convection and ICWs.

5. Due to the magnetospheric convection electric field the strongest precipitating fluxes take place in the nightside MLT sector, and in the low-energy channel (1–50 keV) they reach a magnitude of 3×10^5 cm^{-2} s^{-1} sr^{-1} during the main phase of the storm period. In comparison with the fluxes induced by the convection electric field, the strength of the wave-induced precipitating fluxes, on average, is smaller. The differences are ~5 times in the low-energy channel (1–50 keV) and ~3 times in the high-energy one (50–400 keV). However, it should be noted that during the late recovery phase the approximately equal fluxes of the magnitude 10^4 cm^{-2} s^{-1} sr^{-1} are found in the high-energy channel.

[26] We have demonstrated here only a few preliminary results from the self-consistent RC-ICW model. In future papers we are planning to present results of the entire 2–7 May 1998 storm simulation along with comparisons with wave and ion experimentally obtained data and with the results from semiempirical RC-ICW models.

[27] **Acknowledgments.** This work was supported by National Science Foundation (NSF) grants ATM-9711381, ATM-9710326, and ATM-9800830, and National Aeronautics and Space Administration (NASA) grant NAG5-6976. We also thank Michelle Thomsen and Geoff Reeves for providing LANL data.

[28] Janet G. Luhmann thanks Jerry Goldstein and another referee for their assistance in evaluating this paper.

References

Akhiezer, A. I., I. A. Akhiezer, R. V. Polovin, A. G. Sitenko, and K. N. Stepanov, *Plasma Electrodynamics*, vol. 2, Pergamon, New York, 1975.

Anderson, B. J., K. Takahashi, R. E. Erlandson, and L. J. Zanetti, Pc1 pulsations observed by AMPTE/CCE in the Earth's outer magnetosphere, *Geophys. Res. Lett.*, *17*, 1853–1856, 1990.

Anderson, B. J., R. E. Erlandson, and L. J. Zanetti, A statistical study of Pc 1–2 magnetic pulsations in the equatorial magnetosphere, 1, Equatorial occurrence distributions, *J. Geophys. Res.*, *97*, 3075–3088, 1992a.

Anderson, B. J., K. R. E. Erlandson, and L. J. Zanetti, A statistical study of Pc 1–2 magnetic pulsations in the equatorial magnetosphere, 2, Wave properties, *J. Geophys. Res.*, *97*, 3089–3101, 1992b.

Angerami, J. J., and J. O. Thomas, Studies of planetary atmospheres, 1, The distribution of ions and electrons in the Earth's exosphere, *J. Geophys. Res.*, *69*, 4537–4570, 1964.

Bespalov, P. A., and V. Y. Trakhtengerts, Cyclotron instability of the Earth radiation belts, in *Reviews of Plasma Physics*, vol. 10, edited by M. A. Leontovich, Consultants Bureau, New York, 1986.

Cornwall, J. M., H. H. Hilton, and P. F. Mizera, Observations of precipitating protons in the energy range 2.5 keV < E < 200 keV, *J. Geophys. Res.*, *76*, 5220–5234, 1971.

Ebihara, Y., and M. Ejiri, Simulation study on fundamental properties of the stormtime ring current, *J. Geophys. Res.*, *105*, 15,843–15,860, 2000.

Erlandson, R. E., L. J. Zanetti, T. A. Potemra, L. P. Block, and G. Holmgren, Viking magnetic and electric field observations of Pc 1 waves at high latitudes, *J. Geophys. Res.*, *95*, 5941–5955, 1990.

Farrugia, C. J., et al., Large-scale geomagnetic effects of 4 May 1998, *Adv. Space Res.*, in press, 2001.

Gamayunov, K. V., and G. V. Khazanov, Influence of hot anisotropic ions on properties of nonlinear Alfvén waves, *Plasma Phys. Controlled Fusion*, *37*, 1095–1117, 1995.

Gamayunov, K. V., E. N. Krivorutsky, A. A. Veryaev, and G. V. Khazanov, Saturation of Alfvén oscillations in the ring current region due to generation of lower hybrid waves, *Planet. Space Sci.*, *40*, 477–479, 1992.

Gendrin, R., Consequences of hydromagnetic waves on magnetospheric particle dynamics, *Space Sci. Rev.*, *42*, 515–557, 1985.

Gonzalez, W. D., J. A. Joselyn, Y. Kamide, H. W. Kroehl, G. Rostoker, B. T. Tsurutani, and V. M. Vasyliunas, What is a geomagnetic storm?, *J. Geophys. Res.*, *99*, 5771–5792, 1994.

Iyemori, T., and K. Hayashi, Pc 1 micropulsations observed by Magsat in ionospheric F region, *J. Geophys. Res.*, *94*, 93–100, 1989.

Jordanova, V. K., J. U. Kozyra, and A. F. Nagy, Effects of heavy ions on the quasi-linear diffusion coefficients from resonant interactions with EMIC waves, *J. Geophys. Res.*, *101*, 19,771–19,778, 1996.

Jordanova, V. K., J. U. Kozyra, A. F. Nagy, and G. V. Khazanov, Kinetic model of the ring current-atmosphere interactions, *J. Geophys. Res.*, *102*, 14,279–14,292, 1997.

Jordanova, V. K., C. J. Farrugia, L. Janoo, J. M. Quinn, R. B. Torbert, K. W. Ogilvie, R. P. Lepping, J. T. Steinberg, D. J. McComas, and R. D. Belian, October 1995 magnetic cloud and accompanying storm activity: Ring current evolution, *J. Geophys. Res.*, *103*, 79–92, 1998a.

Jordanova, V. K., C. J. Farrugia, J. M. Quinn, R. M. Thorne, K. W. Ogilvie, R. P. Lepping, G. Lu, A. J. Lazarus, M. F. Thomsen, and R. D. Belian, Effect of wave-particle interactions on ring current evolution for January 10–11, 1997: Initial results, *Geophys. Res. Lett.*, *25*, 2971–2974, 1998b.

Jordanova, V. K., C. J. Farrugia, R. M. Thorne, G. V. Khazanov, G. D. Reeves, and M. F. Thomsen, Modeling ring current proton precipitation by EMIC waves during the May 14–16, 1997, storm, *J. Geophys. Res*, *106*, 7–22, 2001.

Kennel, C. F., and H. E. Petschek, Limit on stably trapped particle fluxes, *J. Geophys. Res.*, *71*, 1–28, 1966.

Khazanov, G. V., T. E. Moore, E. N. Krivorutsky, J. L. Horwitz, and M. W. Liemohn, Lower hybrid turbulence and ponderomotive force effects in space plasmas subjected for large-amplitude low-frequency waves, *Geophys. Res. Lett.*, *23*, 797–800, 1996.

Khazanov, G. V., E. N. Krivorutsky, M. W. Liemohn, and J. L. Horwitz, A model for lower hybrid wave excitation compared with observations by Viking, *Geophys. Res. Lett.*, *24*, 2399–2402, 1997a.

Khazanov, G. V., E. N. Krivorutsky, T. E. Moore, M. W. Liemohn, and J. L. Horwitz, Lower hybrid oscillations in multicomponent space plasmas subjected to ion cyclotron waves, *J. Geophys. Res.*, *102*, 175–184, 1997b.

Khazanov, G. V., K. V. Gamayunov, and M. W. Liemohn, Alfvén waves as a source of lower-hybrid activity in the ring current region, *J. Geophys. Res.*, *105*, 5403–5410, 2000.

Kozyra, J. U., E. G. Shelley, R. H. Comfort, L. H. Brace, T. E. Cravens, and A. F. Nagy, The role of ring current O^+ in the formation of stable auroral red arcs, *J. Geophys. Res.*, *92*, 7487–7502, 1987.

Kozyra, J. U., V. K. Jordanova, R. B. Horne, and R. M. Thorne, Modeling of the contribution of electromagnetic ion cyclotron (EMIC) waves to stormtime ring current erosion, in *Magnetic Storms*, *Geophys. Monogr. Ser.*, vol. 98, edited by B. T. Tsurutani et al., pp. 187–202, AGU, Washington, D. C., 1997.

LaBelle, J., R. A. Treumann, W. Baumjohann, G. Haerendel, N. Sckopke, G. Paschmann, and H. Lühr, The duskside plasmapause/ring current interface: Convection and plasma wave observations, *J. Geophys. Res.*, *93*, 2573–2590, 1988.

LeVeque, R. J., *Numerical Methods for Conservation Laws*, 2nd ed., Birkhäuser Boston, Cambridge, Mass., 1992.

Lyatsky, W. B., and Y. P. Mal'tsev, *The Magnetosphere-Ionosphere Interaction*, Nauka, Moscow, 1983.

Lyons, L. R., and D. J. Williams, *Quantitative Aspects of Magnetospheric Physics*, D. Reidel, Norwell, Mass., 1984.

Mauk, B. H., Helium resonance and dispersion effects on geostationary Alfvén/ion cyclotron waves, *J. Geophys. Res.*, *87*, 9107–9119, 1982.

Omura, V., M. Ashour-Abdalla, R. Gendrin, and K. Quest, Heating of thermal helium in the equatorial magnetosphere: A simulation study, *J. Geophys. Res.*, *90*, 8281–8292, 1985.

Potter, D., *Computational Physics*, John Wiley, New York, 1973.

Rairden, R. L., L. A. Frank, and J. D. Craven, Geocoronal imaging with Dynamics Explorer, *J. Geophys. Res.*, *91*, 13,613–13,630, 1986.

Rasmussen, C. E., S. M. Guiter, and S. G. Thomas, Two-dimensional model of the plasmasphere: Refilling time constants, *Planet. Space Sci.*, *41*, 35–52, 1993.

Sheldon, R. B., and D. C. Hamilton, Ion transport and loss in the Earth's quiet ring current, 1, Data and standard model, *J. Geophys. Res.*, *98*, 13,491–13,508, 1993.

Simons, S. L., P. H. Reiff, R. W. Spiro, D. A. Hardy, and H. W. Kroehl, A comparison of precipitating electron energy flux on March 22, 1979

with an empirical model: CDAW 6, *J. Geophys. Res.*, *90*, 2727–2734, 1985.

Stern, D. P., The motion of a proton in the equatorial magnetosphere, *J. Geophys. Res.*, *80*, 595–599, 1975.

Tanaka, M., Simulations of heavy ion heating by electromagnetic ion cyclotron waves by proton temperature anisotropies, *J. Geophys. Res.*, *90*, 6459–6468, 1985.

Volland, H., A semiempirical model of large-scale magnetospheric electric fields, *J. Geophys. Res.*, *78*, 171–180, 1973.

Yanenko, N. N., *The Method of Fractional Steps: The Solution of Problems of Mathematical Physics in Several Variables*, Springer-Verlag, New York, 1971.

Young, D. T., S. Perraut, A. Roux, C. de Villedary, R. Gendrin, A. Korth, G. Kremser, and D. Jones, Wave-particle interactions near Ω_{He^+} observed on GEOS 1 and 2, 1, Propagations of ion cyclotron waves in He^+-rich plasma, *J. Geophys. Res.*, *86*, 6755–6772, 1981.

K. V. Gamayunov and E. N. Krivorutsky, Geophysical Institute, University of Alaska, Fairbanks, 903 Koyukuk Dr., P. O. Box 757320, Fairbanks, AK 99775, USA. (gamayunov@gi.alaska.edu; krivorut@gi.alaska. edu)

V. K. Jordanova, Space Science Center, University of New Hampshire, Durham, NH 03824, USA. (vania.jordanova@unh.edu)

G. V. Khazanov, Space Science Department, National Space Science and Technology Center, NASA Marshall Space Flight Center, 320 Sparkman Drive, Huntsville, AL 35805, USA. (george.khazanov@msfc.nasa.gov)